

^{91}Zr NMR in non-stoichiometric zirconium hydrides, ZrH_x ($1.55 \leq x \leq 2$)

K. Niedźwiedź, B. Nowak* and O. J. Żogał

Institute of Low Temperature and Structure Research, Polish Academy of Sciences, PO Box 937, 50-950 Wrocław 2 (Poland)

(Received September 11, 1992)

Abstract

^{91}Zr nuclear magnetic resonance (NMR) has been observed in f.c.c. (δ phase) and f.c.t. (ϵ phase) ZrH_x ($1.55 \leq x \leq 2$) in the temperature range 150–294 K. A systematic increase in the linewidth with decreasing hydrogen content was observed and possible sources of the line broadening are discussed. Both the line shapes and ^{91}Zr Knight shifts were found to be temperature independent. In the ϵ phase the shift, which results from competition between positive d-orbital and negative d-core polarization contributions, was found to be concentration dependent, exhibiting a local minimum near $x=1.8$. This behaviour is consistent with the hydrogen spin–lattice relaxation rate measured previously by several authors and confirms the existence of a local maximum in the electronic density of states at the Fermi level, $N(E_F)$, at $x=1.8$ in the ZrH_x system. In the δ phase the shift is about 85% larger than in the ϵ phase and its magnitude results mainly from d-orbital interactions.

1. Introduction

In the zirconium–hydrogen system for the concentration range $1.5 \leq x \leq 2.0$ where x is the H:Zr ratio, there are two hydride phases stable under normal conditions. The cubic (f.c.c.) δ phase and tetragonal (f.c.t.) ϵ phase exist for $1.55(5) \leq x \leq 1.65(2)$ and $1.74(2) \leq x \leq 2.0$ respectively. A mixed δ and ϵ phase region lies between $x=1.65(2)$ and $1.74(2)$. In addition to these phases, the γ phase monohydride, presumably metastable, exists. It is most frequently observed for $x \leq 1.55$. The phase boundaries given above are the result of a compilation of phase diagram information from several sources by Bowman *et al.* [1], though the agreement between the various sources is not always completely satisfactory. Petrunin *et al.* [2], for example, reported the coexistence of two (δ and ϵ) phases even for D:Zr=1.82. Also, Beck [3] observed the δ phase together with the ϵ phase for H:Zr=1.81. Some of these discrepancies are most likely due to possible oxygen contamination.

Investigations of the electrical and magnetic properties of zirconium hydrides have shown the metallic nature of the hydrides and their weak paramagnetism [4, 5]. The electrical conduction in the δ phase is mainly due to holes, whereas in the ϵ phase the major conduction is via electrons [4]. The magnetic susceptibility, which is nearly stoichiometry independent in the δ

phase, decreases significantly with increasing hydrogen content in the ϵ phase [5]. Band theory calculations of the electronic density of states, $N(E_F)$, have been limited to the stoichiometric composition ZrH_2 [6–8]. They predict a sharp $N(E_F)$ peak in hypothetical cubic ZrH_2 and a much lower (about one-half of that for the cubic dihydride) $N(E_F)$ value for tetragonal ZrH_2 [7, 8].

Both the proton spin–lattice relaxation times (T_1) and the Knight shifts (K) have been measured in non-stoichiometric ZrH_x [1, 5, 9, 10]. An $N(E_F)$ peak at a hydrogen concentration $x \approx 1.8$ was determined from these studies [1, 5, 9]. In turn, the nuclear magnetic resonance (NMR) of ^{91}Zr nuclei was reported only recently for tetragonal ZrH_2 [11, 12]. The conclusions about the low value of $N(E_F)$ resulting from these studies are in agreement with those of electron band structure calculations. They have also indicated the orbital hyperfine interaction as the dominant contribution to the Knight shift. Also, the combination of ^{91}Zr magic angle spinning (MAS) NMR with conventional pulse Fourier transform NMR allowed the determination of the isotropic and anisotropic parts of the K tensor.

In this study we have extended our previous ^{91}Zr NMR measurements to non-stoichiometric compositions of the hydrides in the Zr–H system, including both δ and ϵ phases. The results of these studies will be compared with other available data describing their electronic properties.

*Author to whom correspondence should be addressed.

2. Experimental details

The ZrH_x samples were prepared by exposing crystal bars of zirconium iodide to hydrogen gas obtained by thermal decomposition of TiH_2 . Before hydrogenation the metal was heated to 600 °C under vacuum. At this temperature gaseous hydrogen was introduced into the reactor vessel. The absorption was performed at a hydrogen pressure lower than 1 atm, the temperature being slowly reduced to room temperature. The hydrogen concentration in the samples was determined by the amount of absorbed gaseous H_2 . The estimated accuracy of the H:Zr ratios is ± 0.02 . All hydrides were ground in a helium atmosphere glove-box and the powders subsequently annealed in vacuum for 60 h at 430 °C, at which temperature no thermal decomposition was observed. After each annealing had been completed, the ZrH_x samples for the NMR experiments were sealed off in evacuated glass tubes (outer diameter 5 mm). A small fraction of each sample was mixed with silicone oil to prevent oxidation and immediately analysed in a Dron 1.5 X-ray diffractometer using $\text{Cu K}\alpha$ radiation. No differences were observed in the diffraction patterns recorded again a few days later on the same samples. The compositions of the samples used in this work and their lattice parameters determined at 294 K are given in Table 1. The ^{91}Zr NMR measurements were made at a resonance frequency of 27.9 MHz using a Bruker MSL 300S spectrometer equipped with B-VT 1000E temperature controller. The temperature was varied between 150 and 294 K. The broadening of the resonance lines was so large in our powdered ZrH_x samples with $x < 2$ that the observation of the free-induction decays was difficult. Therefore all measurements were carried out using spin echoes produced by a sequence of two equal-width pulses. The spectra are the Fourier transforms of the spin echo signals. Depending on the

hydrogen concentration in the sample investigated, up to about 60000 scans were required to achieve an adequate signal-to-noise ratio. The ^{91}Zr Knight shifts were measured with respect to the ^{91}Zr signal in BaZrO_3 , whose chemical shift is 208.1 ppm [13].

3. Results and discussion

The ^{91}Zr NMR spectra of ZrH_x hydrides are found to be very sensitive to hydrogen concentration (Figs. 1 and 2). The linewidths and Knight shifts were temperature independent in the temperature range 150–294 K. In the f.c.t. ϵ phase the narrowest signal is observed for stoichiometric ZrH_2 , for which the strongest tetragonal deformation is observed. With decreasing hydrogen concentration the tetragonal deformation decreases, but at the same time the number of hydrogen vacancies increases and the electric field gradient (EFG) as well as the anisotropic Knight shift at the Zr site

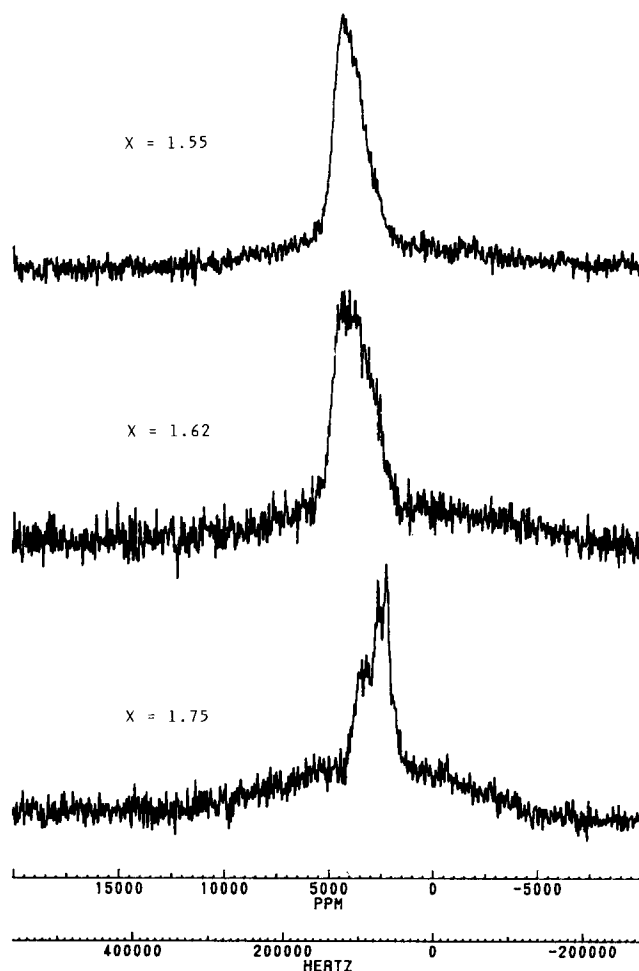


Fig. 1. Absorption spectra of ^{91}Zr resonance for various hydrogen concentrations x in ZrH_x recorded at 27.9 MHz. The spectra are the Fourier transforms of the spin echo signals produced by two equal-width pulses (typically 1–2 μs).

TABLE 1. Sample compositions, X-ray and ^{91}Zr NMR data

Composition	Phase(s) observed	Lattice parameters (\AA)		Knight shift ^a (%)
		a_0	c_0	
$\text{ZrH}_{2.00}$	ϵ	4.975(3)	4.447(3)	0.246(5) ^b
$\text{ZrH}_{1.94}$	ϵ	4.975(3)	4.447(3)	0.242(5)
$\text{ZrH}_{1.88}$	ϵ	4.966(3)	4.449(3)	0.235(5)
$\text{ZrH}_{1.81}$	ϵ	4.951(3)	4.478(3)	0.215(5)
$\text{ZrH}_{1.75}$	ϵ	4.929(5)	4.521(5)	0.230(5)
$\text{ZrH}_{1.62}$	δ	4.780(2)	—	0.43 (approx.)
	ϵ	4.887(3)	4.585(5)	
$\text{ZrH}_{1.55}$	δ	4.776(3)	—	0.430(10)

^aKnight shifts are referred to maximum intensity of absorption line (see text); ^bthe K_{iso} and K_{ax} values for this sample are given in ref. 12; numbers in parentheses are estimated uncertainties in the last quoted digit.

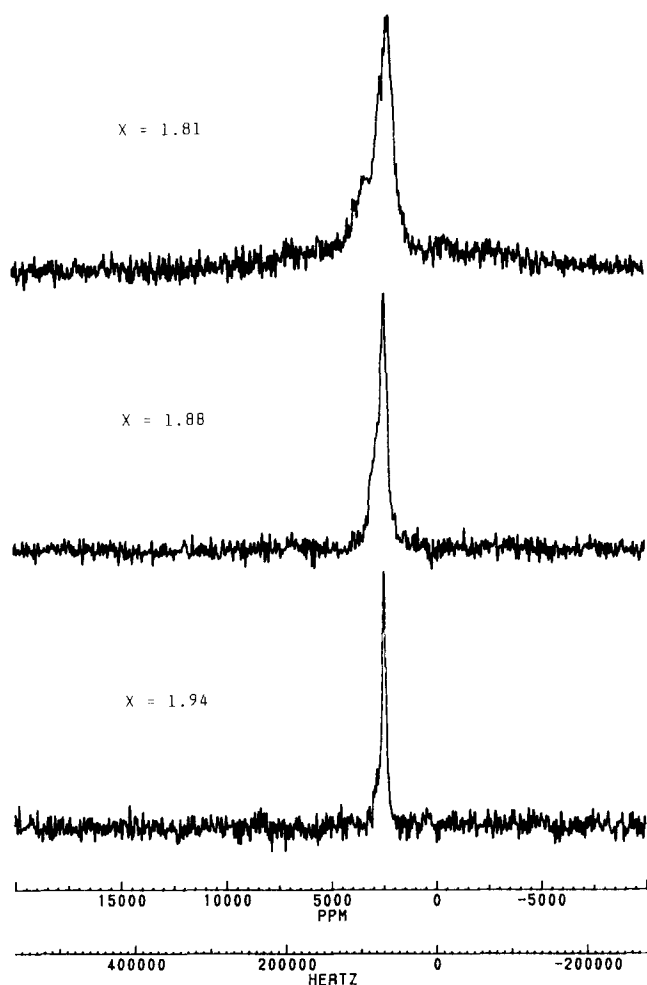


Fig. 2. Absorption spectra of ^{91}Zr resonance for various hydrogen concentrations x in ZrH_x . Experimental conditions as in Fig. 1.

generated by the non-cubic hydrogen nearest neighbours become more important. The broadest signal is observed in $\text{ZrH}_{1.55}$ (δ phase) despite the long-range cubic symmetry of the crystal lattice. It is thus evident that local rather than bulk symmetry is essential. Similar effects were also observed in $^{47,49}\text{Ti}$ NMR studies of TiH_x [14] and $\text{Ti}_{1-y}\text{V}_y\text{H}_x$ [15]. Usually for non-cubic symmetry, quadrupolar and Knight shift anisotropies may occur together and these effects ought to be treated simultaneously in interpreting the observed spectra. This is particularly important in the case of powder specimens. Both static and MAS ^{91}Zr NMR experiments on stoichiometric ZrH_2 samples [12] clearly indicated that the Knight shift anisotropy determines the line shape and that the quadrupolar interactions in the magnetic field of 7 T can be neglected. Actually, in our spectra of substoichiometric ZrH_x hydrides the presence of a first-order spread in the resonance frequencies of satellite transitions seems to be indicated by the low intensity bumps on both sides of the central $\frac{1}{2} \leftrightarrow -\frac{1}{2}$ transition. The central part of the ^{91}Zr spectra (Figs. 1 and 2) exhibits two characteristic features: (1) an increase in

line broadening with decreasing x ; (2) the spectra for the δ phase are more symmetric than those for the ϵ phase and show a slight asymmetry towards lower frequencies. The dipole-dipole interactions (^{91}Zr - ^{91}Zr and ^{91}Zr - ^1H) are not strong enough to account for the observed broadening and should in fact be weaker for smaller x , contrary to the first observation.

The second feature is also opposite to the second-order quadrupolar effects, which cause a more intense part of the signal at the lower frequency edge (at the $\theta = 41.8^\circ$ singularity, where θ is the angle between the axis of symmetry of a particular crystal or crystallite and the applied magnetic field direction) [16]. Therefore it seems to us that an inhomogeneous Knight shift distribution at the Zr site should be considered as the main source of the observed broadening of the central part of the ^{91}Zr spectra. Actually, such an effect has recently been reported for V and Al solute nuclei in α -Ti [17]. To explain the shape of the ^{51}V and ^{27}Al NMR absorption spectra, a gaussian distribution of the isotropic Knight shift (K_{iso}) has been assumed. A gaussian full width $2 [2 \ln 2 \langle (\Delta K)^2 \rangle]^{1/2} = 1.88 \times 10^{-2}\%$ and $3.77 \times 10^{-2}\%$ for Ti-2at.%V and Ti-1at.%Al respectively resulted. Here $\Delta K = K - K_0$, where K_0 is the average value of K_{iso} . In our case a larger width will be necessary to fit the experimental data. This is reasonable, since the deviation from stoichiometry of the zirconium hydrides studied here is larger than that of the Ti alloys mentioned above.

The observed asymmetry of the central line cannot be unambiguously explained by a second-order quadrupole effect or a Knight shift anisotropy (or both), since our experiments were carried out at one value of magnetic field ($B_0 = 7.05$ T). Unfortunately, the ^{91}Zr NMR signals for ZrH_x ($x < 2$) were so broad that MAS ($\nu_r = 6$ kHz is our maximum available rotation rate at the moment) was of no benefit. Consequently, the true values of the isotropic part of the Knight shift (K_{iso}) could not be determined very precisely. Nevertheless, to characterize the dependence of the position of the resonance line (Knight shift) on the hydrogen concentration x in the ϵ phase of ZrH_x , we have used the positions of the maxima on the recorded absorption resonance lines as the shift values. These values are thus slightly underestimated with respect to the true values of K_{iso} , but give a correct trend of the zirconium resonance shift as a function of the hydrogen concentration (Fig. 3).

Band structure calculations for cubic ZrH_2 [6] and decomposition of the electron density of states into its partial wave components show that the metal d-states are largely dominant at the Fermi energy E_F , while the s- and p-state contributions at E_F are vanishingly small. Although no such data are reported for tetragonal ZrH_2 and substoichiometric tetragonal ZrH_x with $x < 2$,

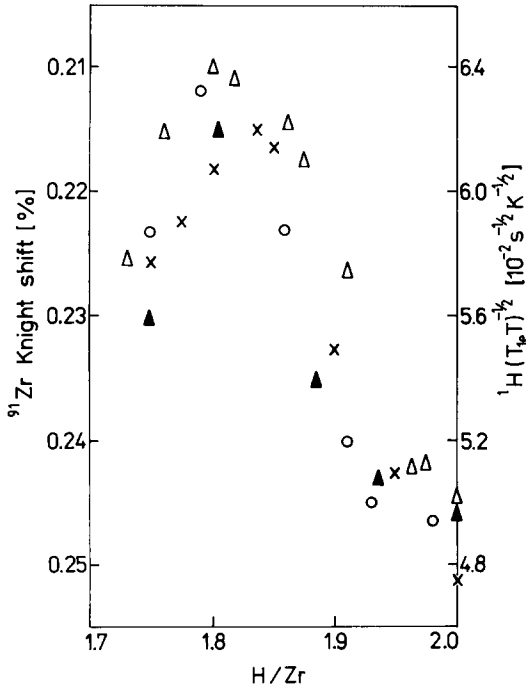


Fig. 3. Concentration dependence of ^{91}Zr Knight shift (\blacktriangle) measured at peak position in f.c.t. ϵ phase of ZrH_x . For comparison the $^1\text{H} (T_{1e}T)^{-1/2}$ value vs. hydrogen concentration is also plotted: \circ , data from ref. 10; \times , data from ref. 5; Δ , data from ref. 9.

we do not expect substantial changes in the s- and p-densities of states. Thus it is assumed that the expansion of the conduction electron wavefunctions at the Fermi level can be limited to $l=2$ atomic functions, *i.e.* $N(E_F) \approx N_d(E_F)$, and the total Knight shift can be represented as the sum of terms arising from d-spin core polarization and d-orbital interactions, which is given by

$$K = K_{\text{cp}} + K_{\text{orb}} + \delta K_{\text{dia}} \\ = (\mu_B N)^{-1} (H_d^{\text{cp}} \chi_d + H_d^{\text{orb}} \chi_{\text{VV}}) + \delta K_{\text{dia}} \quad (1)$$

where μ_B is the Bohr magneton, N is Avogadro's number, H_d^{cp} and H_d^{orb} are the d-core polarization and d-orbital hyperfine fields respectively and χ_d and χ_{VV} are the spin paramagnetic and Van Vleck orbital magnetic susceptibilities of the partially filled 4d band respectively. The latter contribute to the total magnetic susceptibility according to

$$\chi = \chi_d + \chi_{\text{VV}} + \chi_{\text{dia}} \quad (2)$$

where χ_{dia} represents the core diamagnetic susceptibility. Finally, δK_{dia} is the diamagnetic contribution to the zirconium Knight shift and reflects the difference in 4d electron shell occupancy between the reference and the hydride. The χ_d and χ_{VV} contributions can be concentration dependent, *i.e.* vary with x in ZrH_x . However, the hyperfine fields H_d^{cp} and H_d^{orb} as well as δK_{dia} and χ_{dia} can be assumed to be independent of x to a good approximation. Qualitatively, since $H_d^{\text{orb}} > 0$, H_d^{cp}

and $\delta K_{\text{dia}} < 0$, the experimental values of the Knight shifts are the result of the partial cancellation between positive d-orbital and negative d-core plus diamagnetic shifts. A quantitative partitioning of the shift and susceptibility data is unfortunately not possible in our case because the magnitudes of δK_{dia} and χ_{dia} cannot be estimated with sufficient accuracy. Despite this, in Fig. 3 we have plotted the concentration dependence of the ^{91}Zr Knight shift of the ϵ phase of ZrH_x together with the proton $(T_{1e}T)^{-1/2}$ values obtained by several authors, where T is the absolute temperature and T_{1e} is the electronic contribution to the proton spin-lattice relaxation time. As can be seen from this figure, the ^{91}Zr Knight shift shows qualitatively the same concentration dependence as the square root of the Korringa product $((T_{1e}T)^{-1/2})$, exhibiting a local maximum of that value and a minimum of the ^{91}Zr Knight shift at $\text{H:Zr} \approx 1.81$. In parallel, the total magnetic susceptibility of the ϵ phase of ZrH_x generally decreases with increasing hydrogen content, displaying a small local maximum at $\text{H:Zr} \approx 1.83$ [5]. Assuming that the s-spin contribution to the proton Korringa product is vanishingly small, the hydrogen concentration dependence of this product is caused primarily by changes in the d-spin electron density of states, $N_d(E_F)$, since $(T_{1e}T)^{-1/2} = C_d N_d(E_F)$, where C_d includes an appropriate hyperfine field. Because $\chi_d \propto N_d(E_F)$, we conclude also that the concentration dependences of the ^{91}Zr Knight shift and magnetic susceptibility are dominated by the variation in the d-spin susceptibility.

Using the magnetic susceptibility data of Bowman *et al.* [5] and our Knight shift values, we have plotted K vs. χ with x as an implicit parameter in Fig. 4. The slope of the so-obtained dependence is negative. However, the hyperfine field (-26 kOe) resulting from it is significantly smaller than that expected (-219 kOe)

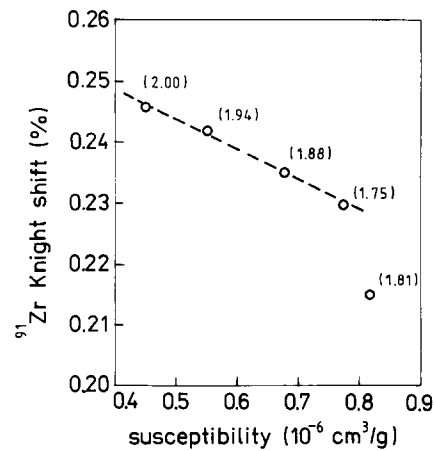


Fig. 4. ^{91}Zr Knight shift K vs. magnetic susceptibility χ , with hydrogen concentration as the implicit parameter, in f.c.t. ϵ phase of ZrH_x . $\chi(x)$ was taken from the work of Bowman *et al.* [5]. Numbers in parentheses represent the hydrogen concentration.

from the core-polarization interaction only. This indicates that in the ϵ phase the orbital susceptibility χ_{VV} decreases with increasing hydrogen content too. The deviation from linear dependence observed for $\text{H}:\text{Zr}=1.81$ is caused by the dominant contribution of the core-polarization interaction, in agreement with postulated peak in the Fermi level density of states near $x=1.8$ [1].

For $\text{ZrH}_{1.55}$ (δ phase) the ^{91}Zr Knight shift and magnetic susceptibility [5] are clearly larger than those observed for the ϵ phase. On the other hand, the electron density of states resulting from the measured proton Korringa product [1] is smaller than that for the ϵ phase. Taking into account the above facts, we may conclude that the excess of the Knight shift and magnetic susceptibility in $\text{ZrH}_{1.55}$ is mainly due to an increased value of the orbital magnetic susceptibility.

References

- 1 R. C. Bowman Jr., E. L. Venturini, B. D. Craft, A. Attalla and D. B. Sullenger, *Phys. Rev. B*, **27** (1983) 1474.
- 2 V. F. Petrunin, V. P. Glazkov, V. I. Savin, V. A. Somenkov, V. K. Fedotov, S. Shil'shteyn and S. V. Marchenko, *Fiz. Met. Metalloved.*, **46** (1978) 206.
- 3 R. J. Beck, *Am. S. M. Trans. Q.*, **55** (1962) 546.
- 4 P. W. Bickel and T. G. Berlincourt, *Phys. Rev. B*, **2** (1970) 4807.
- 5 R. C. Bowman Jr., B. D. Craft, J. S. Cantrell and E. L. Venturini, *Phys. Rev. B*, **31** (1985) 5604.
- 6 M. Gupta and J. P. Burger, *Phys. Rev. B*, **24** (1981) 7099.
- 7 A. C. Switendick, *J. Less-Common Met.*, **101** (1984) 191.
- 8 A. C. Switendick, *J. Less-Common Met.*, **103** (1984) 3091.
- 9 C. Korn, *Phys. Rev. B*, **28** (1983) 95.
- 10 J. W. Han, D. R. Torgeson, R. G. Barnes and D. T. Peterson, *Phys. Rev. B*, **44** (1991) 12353.
- 11 O. J. Żogał, B. Nowak and K. Niedźwiedz, *Solid State Commun.*, **80** (1991) 601.
- 12 O. J. Żogał, B. Nowak and K. Niedźwiedz, *Solid State Commun.*, **82** (1992) 351.
- 13 J. S. Hartman, F. P. Koffyberg and J. A. Ripmeester, *J. Magn. Reson.*, **91** (1991) 400.
- 14 S. D. Goren, C. Korn, H. Rieseemeier, E. Rössler and K. Lüders, *Phys. Rev. B*, **34** (1986) 6917.
- 15 B. Nowak, O. J. Żogał and K. Niedźwiedz, *J. Alloys Comp.*, **189** (1992) 141.
- 16 I. D. Weisman, L. J. Swartzendruber and L. H. Bennett, in E. Passaglia (ed.), *Techniques of Metals Research*, Vol. VI, Part 2, Wiley, New York, 1973, p. 219.
- 17 L. H. Chou and T. J. Rowland, *Phys. Rev. B*, **45** (1992) 11580.